A temperature modulation photonic crystal Mach-Zehnder interferometer composed of copper oxide high-temperature superconductor

Ting-Hang Pei and Yang-Tung Huang

Citation: Journal of Applied Physics **101**, 084502 (2007); doi: 10.1063/1.2714649
View online: http://dx.doi.org/10.1063/1.2714649
View Table of Contents: http://scitation.aip.org/content/aip/journal/jap/101/8?ver=pdfcov
Published by the AIP Publishing

A temperature modulation photonic crystal Mach-Zehnder interferometer composed of copper oxide high-temperature superconductor

Ting-Hang Pei[a] and Yang-Tung Huang
Department of Electronics Engineering and Institute of Electronics, National Chiao Tung University, 1001 Ta-Hsueh Road, Hsinchu, Taiwan 300, Republic of China

(Received 30 August 2006; accepted 24 January 2007; published online 18 April 2007)

A tunable Mach-Zehnder interferometer with a two-dimensional photonic crystal structure using copper oxide high-temperature superconductor is proposed. This photonic crystal is composed of rods of which axes are perpendicular to the two-dimensional anisotropic copper oxide plane. By tuning the temperature of the superconductor, the refractive index of the superconductor as well as the photonic band gap can be changed. The photonic band structures of two-dimensional photonic crystals composed of the superconductor are calculated by using the plane-wave expansion method, and interference properties are investigated by using the finite-difference time-domain method. For our designed photonic crystal Mach-Zehnder interferometer, the simulation results show that the light transmission can be modulated from 92.7% to 1.4% with different temperature distributions.
 [DOI: 10.1063/1.2714649]

I. INTRODUCTION

It is well known that photonic crystals (PCs) formed with dielectric periodic structures may have photonic band gaps (PBGs).[1,2] The Bloch theorem can be applied to describe the photonic band structure for electromagnetic wave propagation in a photonic crystal, which is very analogous to the electron band structure for electron transportation in a solid. The electromagnetic wavelength of the propagating light in PCs, which we are interested in, is often on the order of the lattice spacing. Utilizing the properties of photonic band gaps, the light can be confined within the point and line defects. Some applications of photonic crystal waveguides that can redirect light extreme efficiently around sharp corners have been developed in two-dimensional and three-dimensional structures.[3–6] Integrated optical devices based on PCs become more and more attractive, and theoretical analysis has shown the possibility of high transmission efficiency in these devices.[5,6]

Photonic band structures (PBSs) strongly depend on refractive indices of materials and the geometry of the photonic crystal. Once the material and geometry structure of a PC are constructed, the possible way to change its PBSs is to tune the refractive indices of its constituent materials utilizing the temperature effect, the external electric field effect, the external magnetic field effect, etc.[7–16] For PCs composed of ferroelectric or ferromagnetic materials, PBSs can be tuned by the external electric field effect and the external magnetic field effect.[9,10] The variation of PBSs of liquid-crystal materials controlled by the external electric field or the temperature has also been investigated.[11–16] Another potential material that can be used to tune the PBSs is the superconductor by varying the temperature and the external magnetic field.[17–19]

In this paper we design a tunable PC Mach-Zehnder interferometer composed of copper oxide high-temperature superconductor utilizing the temperature modulation. The Mach-Zehnder interferometer, whose path-length difference of two arms is fixed after it is designed, can be realized as an optical switching device or sensor. In the output the signals from two arms will interfere, and the phases of these two signals can be modulated for a tunable PC Mach-Zehnder interferometer. The interference property of our designed tunable PC Mach-Zehnder interferometer is numerically simulated using the finite-difference time-domain (FDTD) method.

II. THEORETICAL ANALYSIS

The superconductor is strongly sensitive to the temperature and the external magnetic field. However, only the effect of the temperature is discussed in this paper. The two-fluid model is used to describe the electromagnetic response of a typical superconductor without an additional magnetic field,[20] and it describes that the electrons in the superconductor occupy one of two states. One is the superconducting state, in which the superconducting electrons of density $N_s(x,y)$ are paired and transport with no resistance. The other is the normal state, in which the normal conducting electrons of density $N_s(x,y)$ act like normal conducting electrons with a nonzero resistance. Both superconducting and normal conducting electrons coexist in a superconductor when the temperature is lower than the critical temperature. This model also characterizes the performance of high-frequency superconductive devices very well.[21] With this model, we consider the electric field parallel to the z axis (TM mode) for a two-dimensional PC structure in the xy plane. In the presence of an external electric field, superconducting and normal conducting current densities J_{sz} and J_{nz} flowing along the z axis can be expressed by the following set of equations:[22]

$$\frac{\partial J_{sz}(x,y)}{\partial t} = \varepsilon_0 \varepsilon_1(x,y)\omega_p^s(x,y)^2 E_z(x,y), \tag{1a}$$

[a]Electronic mail: thp3000.ee88g@nctu.edu.tw

$$\tau\frac{\partial J_{nz}(x,y)}{\partial t}+J_{nz}(x,y)=\tau\varepsilon_0\varepsilon_1(x,y)\omega_p^n(x,y)^2E_z(x,y). \quad (1b)$$

where $\omega_p^s(x,y)$, $\omega_p^n(x,y)$, and $\lambda(x,y)$ are the plasma frequencies for the superconducting and normal conducting electrons given as

$$\omega_p^s(x,y)=\sqrt{N_s(x,y)e^2/\varepsilon_0\varepsilon_1(x,y)m}=c/\lambda(x,y)\sqrt{\varepsilon_1(x,y)},$$

$$\omega_p^n(x,y)=\sqrt{N_n(x,y)e^2/\varepsilon_0\varepsilon_1(x,y)m}.$$

$\lambda(x,y)$ is the London penetration depth, $\varepsilon_1(x,y)$ is the distribution of the dielectric constant, τ is the relaxation time, c is the wave velocity in free space, and m is the mass of the electron. With a harmonic electric field of frequency ω, J_{sz} and J_{nz} could be expressed as follows:

$$J_{sz}(x,y)=-i\varepsilon_0\varepsilon_1(x,y)\frac{\omega_p^s(x,y)^2}{\omega}E_z(x,y), \quad (2a)$$

$$J_{nz}(x,y)=\varepsilon_0\varepsilon_1(x,y)\frac{\omega_p^n(x,y)^2\tau}{(1+i\omega\tau)}E_z(x,y). \quad (2b)$$

Substituting Eqs. (2a) and (2b) into the wave equation for the electric field parallel to z axis results in the following equation:

$$\frac{\partial^2E_z(x,y)}{\partial x^2}+\frac{\partial^2E_z(x,y)}{\partial y^2}=-\frac{\omega^2\varepsilon_1(x,y)}{c^2}\left[1-\frac{\omega_p^s(x,y)^2}{\omega^2}-\frac{\omega_p^n(x,y)^2\tau}{\omega(1+i\omega\tau)}\right]E_z(x,y)$$
$$=-\frac{\omega^2}{c^2}\varepsilon_s(x,y,\omega)E_z(x,y), \quad (3)$$

where $\varepsilon_s(x,y,\omega)$ is the effective dielectric function given as

$$\varepsilon_s(x,y,\omega)=\varepsilon_1(x,y)\left[1-\frac{\omega_p^s(x,y)^2}{\omega^2}-\frac{\omega_p^n(x,y)^2\tau}{\omega(1+i\omega\tau)}\right]. \quad (4)$$

For high-temperature superconductors (HTSCs), optical characteristics show the anisotropic properties.[19] The electric fields parallel and perpendicular to the c axis feel different dielectric indices. However, Eq. (3) is still valid even for anisotropic materials.[17] When the electric fields are parallel to the c axis, plasma frequencies are in the microwaves and far-infrared regions.[19] In our case, we choose the z axis corresponding to the c axis.

In the superconducting state, the electromagnetic wave can propagate in the range of the London penetration depth, and the London penetration depth is dependent on the temperature T, which can be expressed as $\lambda(T)=\lambda_0/\sqrt{1-(T/T_c)^4}$,[22] where λ_0 and T_c are the value of $\lambda(T)$ at the absolute zero temperature and the critical temperature of the superconductor, respectively. When the temperature is above about 0.8 times the critical temperature, the London penetration depth increases rapidly and approaches infinity as the temperature is close to T_c. $\omega_p^s(x,y)$ strongly depends on the London penetration depth as well as the temperature. Based on the experimental results[23,24] in the far-infrared frequency range we consider here, the small contribution of the normal conducting electrons can be neglected and the plasma frequency $\omega_p^s(x,y)$ can be assumed to be uniform within the rods. Then the third term on the right side of Eq. (4) can be dropped and Eq. (4) becomes

$$\varepsilon_s(x,y,\omega)\approx\varepsilon_1(x,y)\left[1-\frac{\omega_p^s(x,y)^2}{\omega^2}\right], \quad (5)$$

which is known as Drude model.[25] This Drude model can also be applied to PCs constituting metallic components, and is used to calculate photonic band structures.

Kuzmiak *et al.*[26] have dealt with two-dimensional photonic crystal systems containing metallic components. We used his method with plane-wave expansion to calculate the photonic band structures of PCs composed of the superconductor, and the photonic crystal dielectric function was directly expanded in a Fourier series. Using the translation vectors of the Bravais lattices L_x and L_y in the primitive unit cell of the triangular lattice, we can have the relation $\varepsilon_s(x+L_x,y+L_y,\omega)=\varepsilon_s(x,y,\omega)$ due to the periodicity of the dielectric constant in this system. $\varepsilon_s(x,y,\omega)$ can be expanded in a Fourier series on reciprocal lattice vectors G_x and G_y as

$$\varepsilon_s(x,y,\omega)=\sum_{\mathbf{G}}\varepsilon_s(\mathbf{G},\omega)e^{i\mathbf{G}\cdot\mathbf{r}}, \quad (6)$$

where the Fourier coefficient $\varepsilon_s(G_x,G_y,\omega)$ is given by

$$\varepsilon_s(\mathbf{G},\omega)=\frac{1}{a_c}\int\varepsilon_s(x,y,\omega)e^{-i\mathbf{G}\cdot\mathbf{r}}d\mathbf{r}. \quad (7)$$

a_c is the area of a primitive unit cell of the triangular lattice; $\mathbf{G}$ and $\mathbf{r}$ are defined as $G_x\hat{i}+G_y\hat{j}$ and $x\hat{i}+y\hat{j}$, respectively. According to Bloch's theory, the electric field can be expanded in the form

$$E_z(x,y)=\sum_{\mathbf{G}}E_z(\mathbf{k}|\mathbf{G})e^{i(\mathbf{k}+\mathbf{G})\cdot\mathbf{r}}, \quad (8)$$

where $\mathbf{k}=k_x\hat{i}+k_y\hat{j}$ is the wave vector of the electromagnetic waves propagating inside the photonic crystal. Substituting Eqs. (5) and (8) into Eq. (3), we obtain the equation of coefficients $E_z(\mathbf{k}|\mathbf{G})$, which is the matrix eigenvalue problem with respect to frequencies ω. With this matrix eigenvalue problem, the frequencies can be solved at a certain wave vector and the photonic band structure can be obtained.

We also designed a tunable Mach-Zehnder interferometer based on the photonic crystal composed of the superconductor. The finite-difference time-domain (FDTD) method was used to calculate the transmission at the output of the Mach-Zehnder interferometer. The FDTD method of dispersive materials utilizes time-domain auxiliary differential equations (ADEs),[27] which were obtained as Eqs. (1a) and (1b). The computation domain is surrounded by the perfectly matched layers (PMLs). Equations (1a) and (1b) were then discretized in two-dimensional space and time by the Yee-cell technique,[28] and were implemented in a FDTD code by finite differences, centered at time step $n+1/2$ as

$$\frac{J_{sz}|_{i,j}^{n+1}-J_{sz}|_{i,j}^{n}}{\Delta t}=(\varepsilon_0\varepsilon_1\omega_p^s)_{i,j}^2\frac{E_z|_{i,j}^{n+1}+E_z|_{i,j}^{n}}{2}, \quad (9a)$$

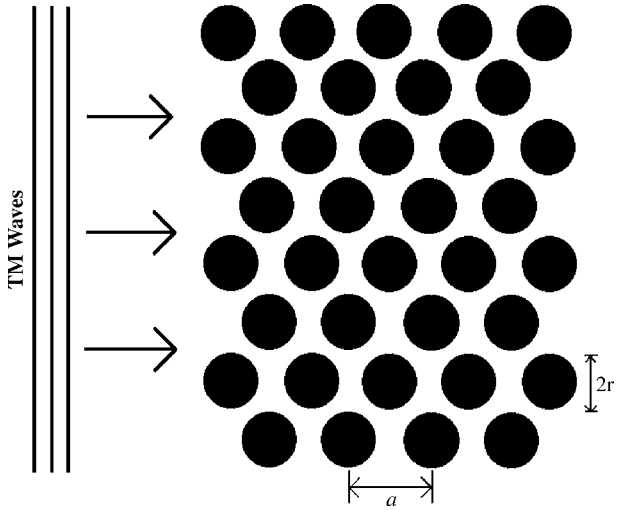

FIG. 1. The cross section of the two-dimensional photonic crystal with a triangular array of superconductor rods.

$$\frac{J_{nz}|_{i,j}^{n+1} - J_{nz}|_{i,j}^{n}}{\Delta t} + \frac{J_{nz}|_{i,j}^{n+1} + J_{nz}|_{i,j}^{n}}{2\tau} = (\varepsilon_0 \varepsilon_1 \omega_p^{n2})_{i,j} \frac{E_z|_{i,j}^{n+1} + E_z|_{i,j}^{n}}{2}, \tag{9b}$$

where the index n denotes the discrete time step, indices i and j denote the discretized grid point in the xy plane, Δt is the time increment, and Δx and Δy are the distances between two neighboring grid points along the x and y directions, respectively.

III. BAND STRUCTURE CALCULATION

In our device design, we used high-T_c superconductor $Bi_{1.85}Pb_{0.35}Sr_2Ca_2Cu_{3.1}O_y$, which has been further investigated.[19,23] Previous study[19] utilized parallel copper oxide HTSC rods to form photonic crystals with square lattices repeating in two-dimensional directions (xy plane). The authors theoretically investigated the tunability of photonic band gaps of two-dimensional photonic crystals by changing temperatures of superconductors and external magnetic fields. The photonic crystal structure we discuss here is composed of superconductor cylinders with triangular lattice in air, as shown in Fig. 1. The electromagnetic wave propagates in the xy plane and has the TM polarization with the electric field parallel to the extended direction of the rod. Adjusting the temperature of superconductors can control the refractive indices of superconductors as well as the photonic band structures of PCs composed of superconductors. When $T \leqslant T_c$ is satisfied, the dependence of the plasma frequency on the temperature is given as[22]

$$\omega_p^s(T) = \omega_p^s(0)/\sqrt{1-(T/T_c)^4}. \tag{10}$$

The London penetration depth of the copper oxide HTSCs that we used is $\lambda = 23\ \mu$m at the reference temperature $T=5$ K, the critical temperature $T_c = 107$ K, and the dielectric constant is $\varepsilon_1 = 12$.[23] When $T=5$ K, we obtain $\omega_p^s/c \approx 1.3\times 10^4\ \text{cm}^{-1}$. We compared PBGs for two different radii of rods $r=0.4a$ and $r=0.2a$ when the periodic lattice constant

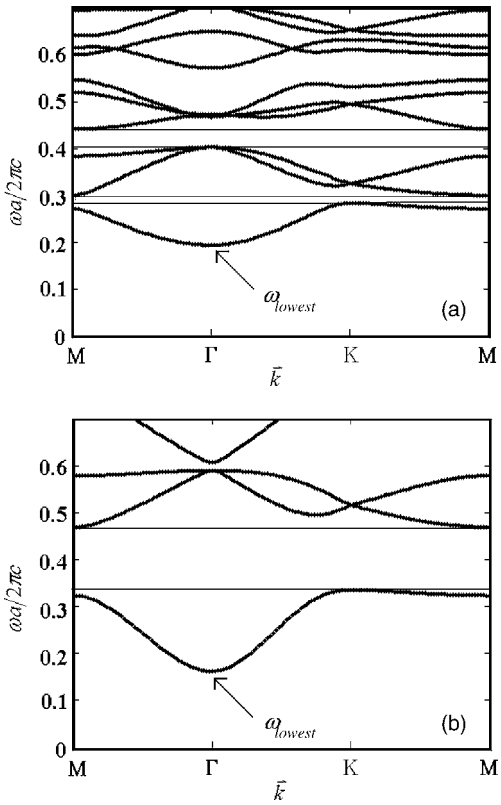

FIG. 2. The band structures of the photonic crystal composed of periodic superconductors at $T=5$ K. (a) $r=0.4a$, (b) $r=0.2a$.

of photonic crystals is $a=100\ \mu$m and the overall temperature is fixed at 5 K. A total of 1849 plane waves was used in our calculations. Figures 2(a) and 2(b) show the photonic band structures along the directions M-Γ, Γ-K, and K-M in the reduced Brillouin zone for radii of rods with $r=0.2a$ and $r=0.4a$, respectively. It can be seen that the photonic bands are much closer and denser for $r=0.4a$ than those for $r=0.2a$. The lowest point of the first band for a metal-like material is above zero frequency, which is not the case in a nondispersive material whose lowest point of the first band is at zero frequency. A photonic band gap exists from zero to a certain frequency ω_{lowest}, which means that the light can propagate in the PC only in the frequency range above ω_{lowest}. In Figs. 2(a) and 2(b) paired horizontal thin lines are drawn to designate the photonic band regions. The second PBG for $r=0.2a$, which is located in the reduced frequency region from 0.33 to 0.47, is much wider than that for $r=0.4a$, which is located in the reduced frequency region from 0.28 to 0.31. The wider the PBG of the PC, the more the applications of PCs.

The band gap regions for different ratios r/a of the rod radius r to the lattice constant a with $a=100\ \mu$m at $T=5$ K, which corresponds to $\omega_p^s a/2\pi c = 0.2$, were calculated, and the lines in Fig. 3 show these band gap regions. The range of the r/a ratio is from 0 to 0.5, and the distance between two neighboring values is 0.02. It can be seen that three PBGs exist below the reduced frequency 0.7. The width of the first PBG increases when r/a increases. It increases slowly when r/a becomes larger and larger. Finally, it saturates and the top of the first PBG is just at the plasma frequency. The

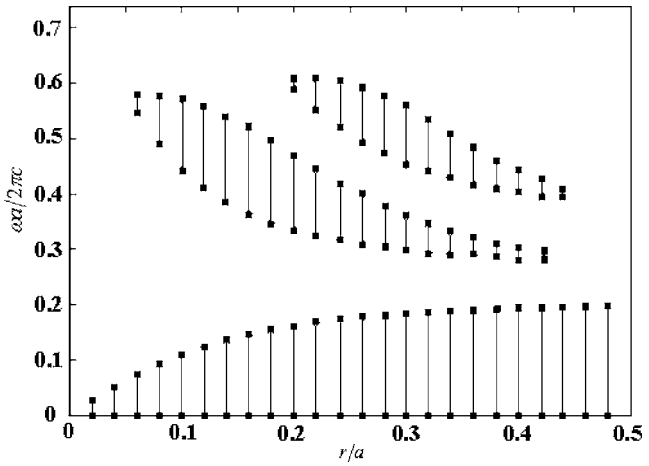

FIG. 3. The band gap regions for different r/a with a is fixed at 100 μm and T=5 K.

possible region of the second PBG in the reduced frequency ranges from 0.27 to 0.57, which can be achieved with r/a between 0.06 and 0.42. It vanishes when r/a is above 0.44. The largest width of the second PBG is about 0.16 in the reduced frequency unit when r/a is between 0.14 and 0.16. The wider PBG allows more defect modes existing in the waveguide region when we design the waveguide on the PC. The other advantage is the tolerance on the fabrication error, since the error of the radius could reduce the PBG. The third PBG exists when r/a is between 0.20 and 0.42. The largest width of the third PBG is about 0.11 when r/a is about 0.3. The influence of the triangular lattice constant a on the PBG was also investigated. We chose the radius of the rod as $r=0.16a$, which has a widest second PBG. The midgaps ω_c of the second band gap with a different lattice constant a for this superconductor photonic crystal at temperatures 5 and 105 K were calculated, and their midgap ratios are shown in Fig. 4. It can be seen that the midgap ratio has changed more than 8% at these two temperatures when the lattice constant is from 20 to 100 μm.

The increase on temperature will cause the increase on the plasma frequency as shown in Eq. (10). The change of the plasma frequency results in the change of the photonic band structure. The 8% change on the midgap is enough to have a large range of change for the propagation character-

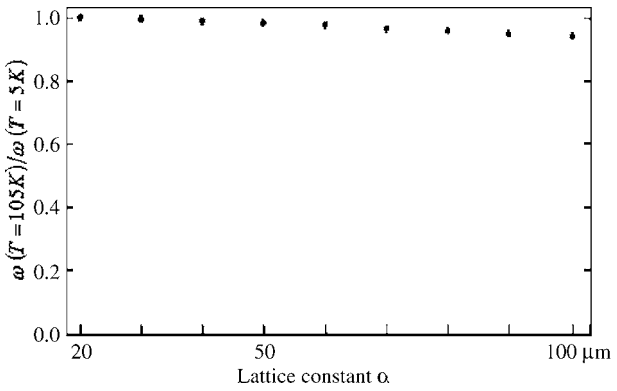

FIG. 4. The midgap ratio between T=5 K and T=105 K when r=0.16a.

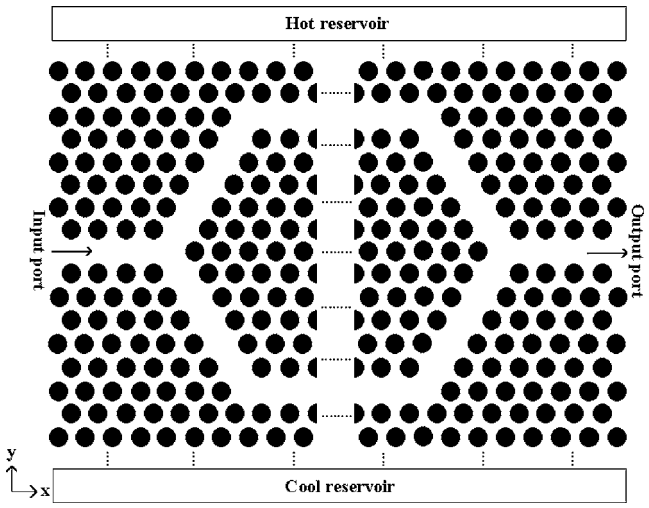

FIG. 5. The Mach-Zehnder interferometer is located between two different temperature reservoirs.

istics of light passing through a photonic crystal device. This lattice constant of 100 μm was then used to design our Mach-Zehnder interferometer device.

IV. DEVICE DESIGN AND CHARACTERISTIC SIMULATION

The designed Mach-Zehnder interferometer device is shown in Fig. 5. The device is laid out in the xy plane with 27 layers in the y direction. The distance of two channels is 12 layers and the length is 30 times the lattice constant. The distance between two channels is equal to $6\sqrt{3}a$. The lattice constant a is 100 μm and the radius r of the rods is 0.16a. The FDTD method was then used to simulate the propagation of electromagnetic waves through the device. The length Δx of each square grid is equal to $a/35$. The total number of the time steps is 120 000 with each step $\Delta t=\Delta x/2c$, where c is light velocity in vacuum. In the FDTD method here, the ADEs described in Sec. II was used to deal with both superconducting and normal conducting electron current densities in superconductors.[26] The TM-polarized continuous wave with a Gaussian profile is launched into the input port. The frequency of the electromagnetic wave is $0.403(2\pi c/a)$ and the corresponding wavelength is 248.1 μm. It is assumed that the device is sandwiched between two reservoirs and both are in stable temperatures, and the temperature distribution is uniformly increasing from the cool reservoir to the hot reservoir through the optical device as shown in the figure. The temperature of the cool reservoir is fixed at 5 K, and the temperature of the hot reservoir is varied from 5 to 105 K. To calculate the photonic band structures in Figs. 2–4, the superconductor currents we considered are only contributed by superconducting electrons, without considering normal electrons. But when the temperature is close to the critical temperature, the normal conducting electron density will increase rapidly, and electrons collide with each other more and more frequently, which will cause the more energy absorption in superconductors. We compared two cases where one includes the normal conducting electrons and the other does not. The relaxation time τ of the normal electrons for

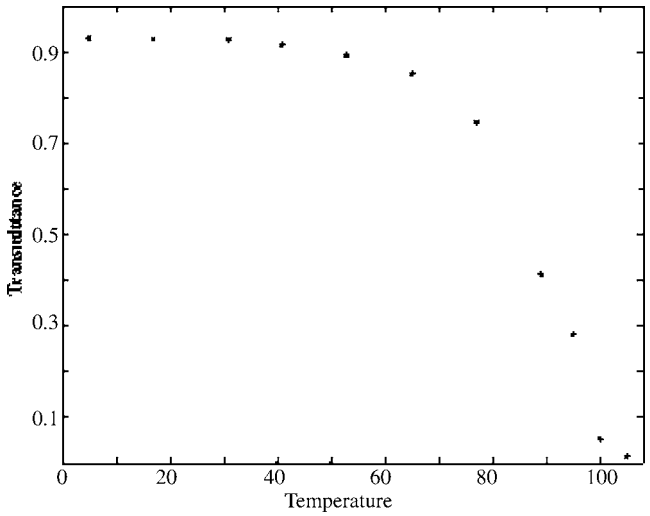

FIG. 6. The transmission of the PC Mach-Zehnder interferometer.

most solid materials is less than 10^{-15} at a temperature above 100 K. It was found that between theses two cases, the difference of the transmission of our device for the temperature from 5 to 105 K we considered is less than 0.02%. So we can discuss the optical properties of the photonic crystals composed of the superconductor with the superconducting electrons only. These corresponding transmissions of the device are shown in Fig. 6. When the temperature of the hot reservoir is above 80 K, the transmission begins to decrease sharply. It can be seen that the transmission can be tuned from about 92.7% to 1.4%, which shows that the optical device we proposed here could serve as an on-off switch in the far-infrared region.

V. CONCLUSION

In conclusion, the two-dimensional photonic crystals using copper oxide high-temperature superconductor (HTSC) with triangle lattice constant of 100 μm can have a large tunability in the photonic band gaps by changing the temperature of the superconductor. The photonic band gap has a 8% change when the temperature is from 5 to 105 K in the superconducting state. The transmission of the photonic crystal Mach-Zehnder interferometer, in which the path length of two channels is 30 times lattice constant, can be tuned from about 92.7% to 1.4%.

ACKNOWLEDGMENT

We are grateful to Dr. C. M. Kwei for offering valuable comments on this work.

[1]S. John, Phys. Rev. Lett. **58**, 2486 (1987).
[2]A. Z. Genack and N. Garcia, Phys. Rev. Lett. **66**, 2064 (1991).
[3]A. Yariv, Y. Xu, R. K. Lee, and A. Scherer, Opt. Lett. **24**, 711 (1999).
[4]M. Bayindir, B. Temelkuran, and E. Ozbay, Phys. Rev. Lett. **84**, 2140 (2000).
[5]S. G. Johnson, P. R. Villeneuve, S. Fan, and J. D. Joannopoulos, Phys. Rev. B **62**, 8212 (2000).
[6]M. Bayindir, E. Ozbay, B. Temelkuran, M. M. Sigalas, C. M. Soukoulis, R. Biswas, and K. M. Ho, Phys. Rev. B **63**, 081107 (2001).
[7]C.-S. Kee and H. Lim, Phys. Rev. B **64**, 121103 (2001).
[8]C.-S. Kee, J.-E. Kim, H. Y. Park, I. Park, and H. Lim, Phys. Rev. B **61**, 15523 (2000).
[9]K. Busch and S. John, Phys. Rev. Lett. **83**, 967 (1999).
[10]A. Figotin, Y. A. Godin, and I. Vitebsky, Phys. Rev. B **57**, 2481 (1998).
[11]C.-S. Kee and H. Lim, Phys. Rev. B **64**, 085114 (2001).
[12]H. Takeda and K. Yoshino, Phys. Rev. E **67**, 056607 (2003).
[13]H. Takeda and K. Yoshino, Phys. Rev. E **67**, 056612 (2003).
[14]H. Takeda and K. Yoshino, Phys. Rev. B **67**, 073106 (2003).
[15]H. Takeda and K. Yoshino, Phys. Rev. E **68**, 046602 (2003).
[16]H. Takeda and K. Yoshino, Phys. Rev. E **70**, 026601 (2004).
[17]W. M. Lee and P. M. Hui, Phys. Rev. B **51**, 8634 (1995).
[18]C. H. Raymond Ooi, T. C. Au Yeung, C. H. Kam, and T. K. Lim, Phys. Rev. B **61**, 5920 (2001).
[19]H. Takeda and K. Yoshino, Phys. Rev. B **67**, 245109 (2003).
[20]M. Tinkham, *Introduction to Superconductivity*, 2nd ed. (McGraw-Hill, New York, 1996).
[21]T. van Duzer and C. W. Truner, *Principle of Superconductive Device and Circuits* (Arnold, London, 1981).
[22]S.-A. Zhou, *Electrodynamics of Solid and Microwave Superconductivity* (Wiley, New York, 1999).
[23]H. Shibata and T. Yamada, Phys. Rev. B **54**, 7500 (1996).
[24]Y. Matsuda, M. B. Gaifullin, K. Kumagai, K. Kadowaki, and T. Mochiku, Phys. Rev. Lett. **75**, 4512 (1995).
[25]G. Grosso and G. Pastori Parravicini, *Solid State Physics* (Academic, New York, 2000).
[26]V. Kuzmiak, A. A. Maradudin, and F. Pincemin, Phys. Rev. B **50**, 16835 (1994).
[27]A. Taflove and S. C. Hagness, *Computational Electrodynamics* (Artech House, Boston, 2000).
[28]K. S. Yee, IEEE Trans. Antennas Propag. **14**, 302 (1966).